Dalton Transactions

Accepted Manuscript

This is an *Accepted Manuscript*, which has been through the RSC Publishing peer review process and has been accepted for publication.

Accepted Manuscripts are published online shortly after acceptance, which is prior to technical editing, formatting and proof reading. This free service from RSC Publishing allows authors to make their results available to the community, in citable form, before publication of the edited article. This *Accepted Manuscript* will be replaced by the edited and formatted *Advance Article* as soon as this is available.

To cite this manuscript please use its permanent Digital Object Identifier (DOI®), which is identical for all formats of publication.

More information about *Accepted Manuscripts* can be found in the **Information for Authors**.

Please note that technical editing may introduce minor changes to the text and/or graphics contained in the manuscript submitted by the author(s) which may alter content, and that the standard **Terms & Conditions** and the **ethical guidelines** that apply to the journal are still applicable. In no event shall the RSC be held responsible for any errors or omissions in these *Accepted Manuscript* manuscripts or any consequences arising from the use of any information contained in them.

TOC graphic

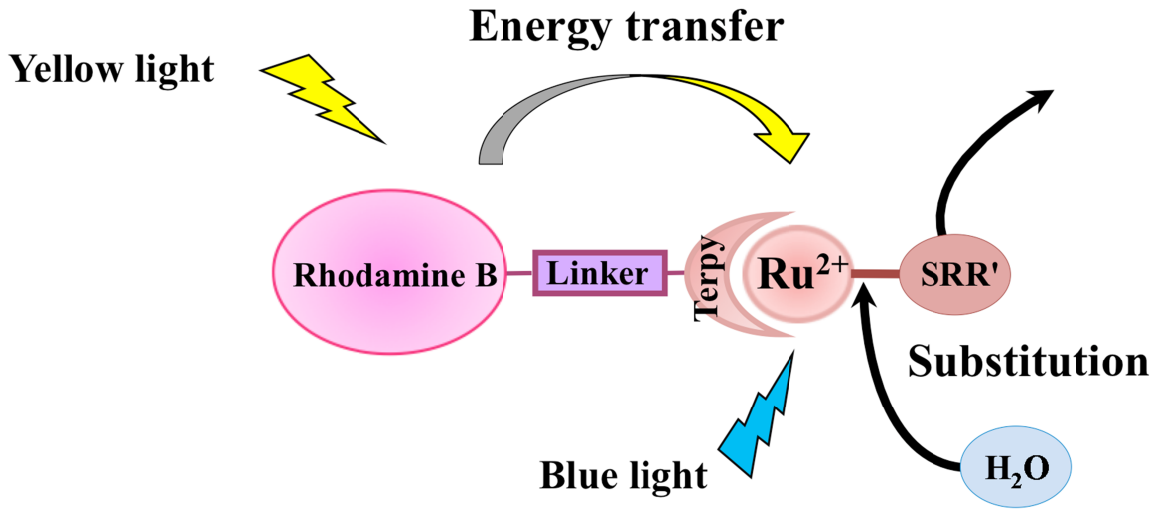

TOC text

A rhodamine dye was covalently attached to a ruthenium complex to enhance the rate of ligand photosubstitution under yellow light irradiation.

Yellow-light sensitization of a ligand photosubstitution reaction in a ruthenium polypyridyl complex covalently bound to a rhodamine dye

Azadeh Bahreman, Jordi-Amat Cuello-Garibo, Sylvestre Bonnet *
Leiden Institute of Chemistry, Gorlaeus Laboratories, Leiden University, P.O. Box 9502, Leiden, 2300 RA, The Netherlands

Abstract

The ruthenium complex $[Ru(terpy)(bpy)(Hmte)]^{2+}$ ($[\mathbf{1}]^{2+}$), where terpy is 2,2';6',2"–terpyridine, bpy is 2,2'-bipyridine, and Hmte is 2-methylthioethan-1-ol, poorly absorbs yellow light, and although its quantum yield for the photosubstitution of Hmte by water is comparable at 570 nm and at 452 nm (0.011(4) *vs.* 0.016(4) at 298 K at neutral pH), the photoreaction using yellow photons is very slow. Complex $[\mathbf{1}]^{2+}$ was thus functionalized with rhodamine B, an organic dye known for its high extinction coefficient for yellow light. Complex $[Ru(Rterpy)(bpy)(Hmte)]^{3+}$ ($[\mathbf{2}]^{3+}$) was synthesized, where Rterpy is a terpyridine ligand covalently bound to rhodamine B *via* a short saturated linker. $[\mathbf{2}]Cl_3$ shows a very high extinction coefficient at 570 nm (44000 $M^{-1}.cm^{-1}$), but its luminescence upon irradiation at 570 nm is completely quenched in aqueous solution. The quantum yield for the photosubstitution of Hmte by water in $[\mathbf{2}]^{3+}$ was comparable to that in $[\mathbf{1}]^{2+}$ at 570 nm (0.0085(6) *vs*. 0.011(4), respectively), which, in combination with the much better photon collection, resulted in a higher photosubstitution rate constant for $[\mathbf{2}]^{3+}$ than for $[\mathbf{1}]^{2+}$. The energy of yellow photons is thus transferred efficiently from the rhodamine antenna to the ruthenium center, leading to efficient photosubstitution of Hmte. These results bring new opportunities for extending the photoactivation of polypyridyl ruthenium complexes towards longer wavelengths.

Introduction

Ruthenium polypyridyl complexes are known for their rich photochemistry, which often requires blue light irradiation.[1-7] In such complexes, photon absorption into a Metal-to-Ligand Charge-Transfer band (^{1}MLCT) typically situated between 400 and 500 nm, leads to the corresponding ^{3}MLCT state *via* intersystem crossing. If the distortion of the octahedral coordination geometry is sufficient to decrease the ligand field splitting energy, further thermal population of the metal-centered excited states (^{3}MC) may result in ligand photosubstitution reactions.[8-11] When performed in aqueous solution, such photoreactions lead to the formation of aqua metal complexes, where one ligand of the coordination sphere has been replaced by one or two water molecules. Recently, this type of photoactive metal complexes have been proposed as light-activated drugs in phototherapy, as the aqua photoproducts may typically interact with biomolecules and lead to significant cytotoxicity, whereas the initial complex may not.[12-21] As has been shown in the literature dealing with Photo Dynamic Therapy (PDT)[22-24] light activation allows for controlling the amount of reactive oxygen species produced locally, which may contribute to limiting toxicity and side effects during chemotherapy. On the other hand, blue light irradiation *in vivo* has a rather limited applicability for PDT since its tissue penetration is low.[25, 26] The fact that the MLCT band of most polypyridyl ruthenium complexes is located in the blue region has been restricting, up to now, real phototherapeutic applications of these complexes. Thus, it is of great interest to make the photoactivation of ruthenium polypyridyl complexes possible also with photons of longer wavelengths, without sacrificing the complex stability in the dark, which is an important requirement in photochemotherapy.

One strategy, recently reviewed by Brewer *et al.*,[27] is to design complexes having their MLCT band at higher wavelengths. Such strategy sometimes lowers the stability of the complexes in the dark, but a few complexes have been published that are reasonably stable in

the dark and photoactive using red light. A second strategy is the coordination of a fluorescent ligand to the ruthenium center in order to sensitize the metal complex with photons of higher wavelength. Mascharak and co-workers [28-30] have used this strategy to bring the sensitization of ruthenium nitrosyl compounds from the UV to the visible region. Typically, direct coordination of the fluorophore to ruthenium promotes merging of the absorption band of both fragments, thus shifting light activation of the metal center towards higher wavelengths.[31] A third, somewhat similar strategy, is to link the fluorophore to the ruthenium complex *via* a non-conjugated linker and to use the "reverse" FRET effect.

Efficient Förster energy transfer (FRET) from a fluorophore to a ruthenium center is typically obtained when the ^{1}MLCT absorption band of the ruthenium complex overlaps with the emission band of the fluorophore. The efficiency of FRET is also related to the distance between the energy donor and the energy acceptor.[32-34] When the maximum of the emission spectrum of the dye is at lower wavelength than the absorption maximum of the ruthenium complex, forward FRET is obtained.[35-37] However, for phototherapeutic application, photoactivation of the ruthenium complex *via* forward FRET, *i.e.,* with photons of low wavelength, is not suitable, and "reverse FRET" from a fluorophore with an emission maximum at a higher wavelength than that of the absorption maximum of the ruthenium moiety, is preferable.[34] Etchenique and co-workers recently introduced this strategy by coordinating a green-emitting, rhodamine B-functionalized nitrile ligand to a chlorido-bis(bipyridine)ruthenium(II) compound. The use of a saturated linker avoided orbital overlap between the organic dye and the ruthenium complex, and green light irradiation was shown to result in photosubstitution of the nitrile ligand, thus releasing the fluorophore from the ruthenium complex.[38]

We report here a new photoactivatable system, in which coupling of the rhodamine B dye is realized at the 4' position of a spectator terpyridine ligand that is not released upon light

irradiation (Figure 1). We recently reported the photosubstitution of the thioether Hmte ligand by an aqua ligand in complex [Ru(terpy)(bpy)(Hmte)]$^{2+}$ (compound [**1**]$^{2+}$, where terpy is 2,2';6',2"-terpyridine, bpy is 2,2'-bipyridine, and Hmte is 2-(methylthio)ethanol).[39] The absorption spectrum of [**1**]$^{2+}$ extends up to 610 nm and slightly overlaps with the emission band of rhodamine B (λ_{em}=570 nm) (Figure 1b). The rhodamine B-functionalized analogue complex [**2**]$^{3+}$ (Figure 1a and 1c) may thus allow energy transfer from the fluorophore to the ruthenium center to occur, thus leading to efficient ligand photosubstitution. The high extinction coefficient of the organic dye may allow for more efficient photon collection and thus faster photosubstitution of Hmte when excited near 600 nm, compared to complex [**1**]$^{2+}$. In this work, the rate and quantum yield for the photosubstitution of Hmte in the analogous ruthenium complexes [**1**]$^{2+}$ and [**2**]$^{3+}$ are compared upon both yellow (570 nm) and blue (450 nm) light irradiation, in order to investigate the efficiency of photosensitization on the Ru-based ligand exchange process.

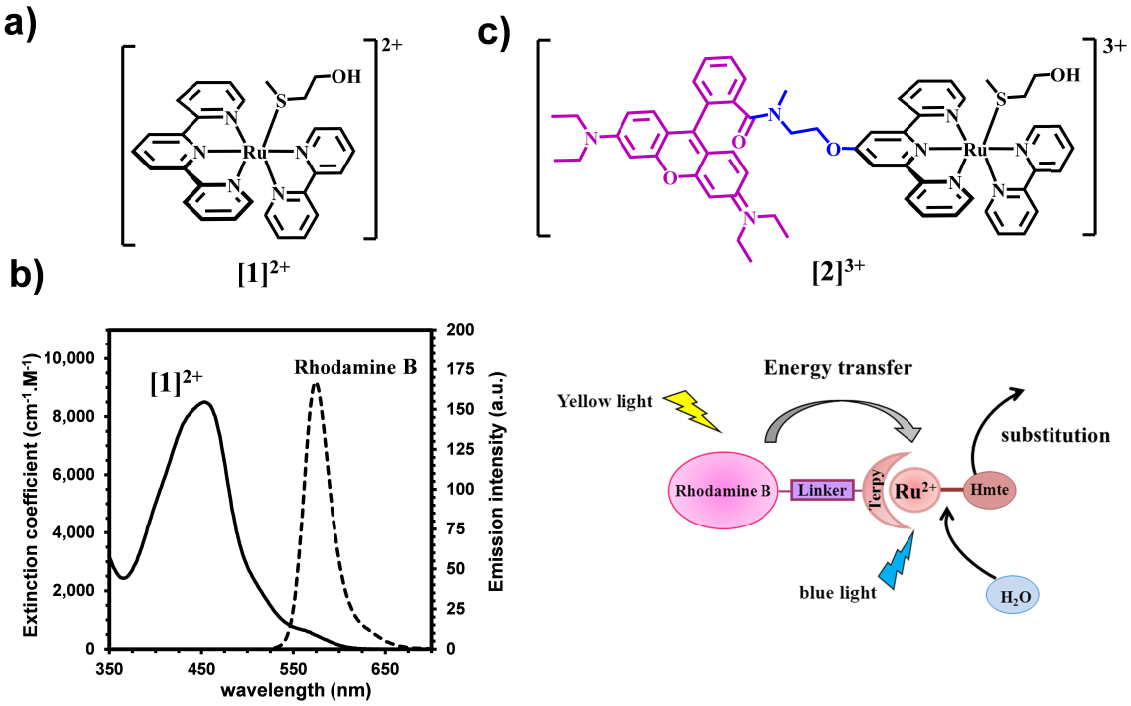

Figure 1. a) Chemical structure of [Ru(terpy)(bpy)(Hmte)]$^{2+}$ ([**1**]$^{2+}$). b) Absorption spectrum of compound [**1**]$^{2+}$ (left axis) and emission spectrum of rhodamine B (right axis). c) Chemical

structure of the rhodamine B-functionalized ruthenium complex [**2**]$^{3+}$ and photochemical scheme.

Results

Synthesis. In order to couple a rhodamine B molecule to the 4' position of the 2,2';6',2"-terpyridine (terpy) ligand an ethanolamine linker may seem at first sight appropriate. However, in basic conditions the secondary amide bond resulting from coupling between the primary amine of ethanolamine and the carboxylic acid of rhodamine B, cyclizes to a spirolactame, which leads to quenching of the fluorescence of the dye.[40, 41] Thus, a secondary amine, 2-methylaminoethanol, was used instead, because the resulting tertiary amide cannot be deprotonated and does not cyclize into the spiro compound. The synthetic route towards ligand [**4**]Cl is shown in Scheme 1. In the first step, a literature procedure was modified[42] to substitute the chloride substituent of 4'-chloro-2,2';6',2"-terpyridine by 2-methylaminoethanol using KOH as a base, to form compound **3**. Two structural isomers, compounds **3** (O-bound) and **3'** (N-bound) (Scheme 1 and Figure S1) can be formed depending on the amount of base, on the temperature, and on the reaction time. By using a low amount of KOH (2.8 eq) and short reaction times no side product **3'** was detected by ^{1}H NMR of the crude product, and compound **3** could be further functionalized.

In the second step, rhodamine B was coupled to **3** following a modified literature procedure [43] involving the acid chloride of rhodamine B and **3** using Et_3N as a base in acetonitrile. After precipitation from water using PF_6^- as a counter ion, full water solubility was recovered by anion exchange to Cl^- using an anion exchange resin. Column chromatography on silica gel allowed removing the unreacted rhodamine B to afford compound [**4**]Cl as a purple solid with an overall yield of 31%. The UV-vis spectrum of [**4**]Cl in water (Figure 2a and Table 1) showed a red shift of about 14 nm (λ_{abs}=569 nm) compared to rhodamine B.

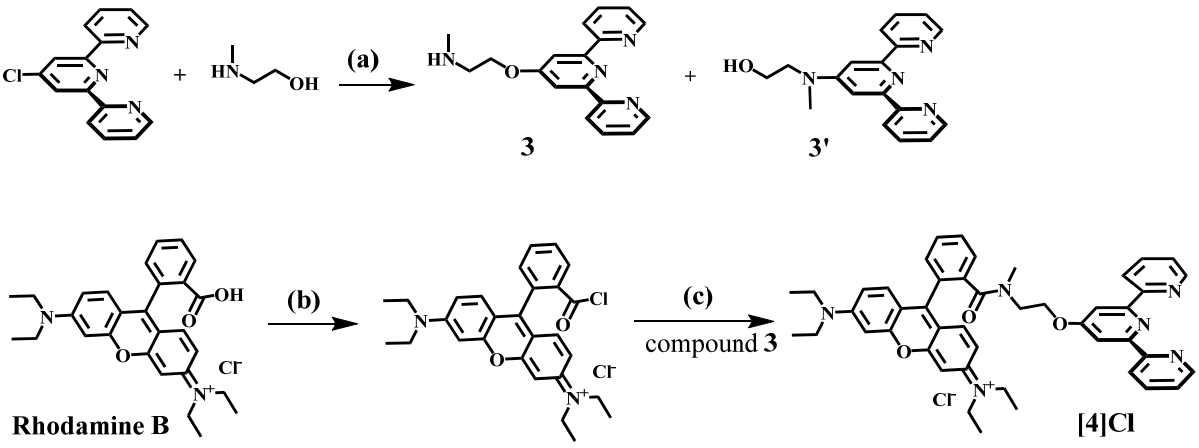

Scheme 1. Synthetic procedure towards compound **3** and [**4**]Cl. (a) KOH, DMSO (dry), heating at 60 °C for 3 h, overnight at R.T. Yield of **3**: 87% (b) $POCl_3$, $C_2H_4Cl_2$ (dry), reflux, 5 h. (c) I: Et_3N, CH_3CN (dry), reflux, 14h, II: KPF_6 in water, III: chloride exchange DOWEX resin, acetone:H_2O (1:1), 4 h, r.t. Yield: 31% (from compound **3**).

Adapting known synthetic procedures[39, 44, 45] the ruthenium complex [**2**]Cl_3 was synthesized as shown in Scheme 2. Refluxing a mixture of ligand [**4**]Cl with $RuCl_3 \cdot 3H_2O$ in methanol resulted in the paramagnetic complex [**5**]Cl. Product formation was followed by TLC and the final product was characterized by paramagnetic ^{1}H NMR and ESI-MS spectrometry. The unpaired electron of the Ru(III) complex generates short relaxation times, which shields the ^{1}H-^{1}H coupling and thus results in broad NMR signals. This effect is significant for hydrogen atoms of the terpyridine moiety in [**5**]Cl that are close to the paramagnetic ruthenium(III) center. Highly upfield-shifted signals were observed in methanol-d4 at −1.43 ppm, −10.26 ppm, −10.71 ppm and −35.94 ppm for T33'', T44'', T55'', or T66''. T3' and T5' are more remote from the paramagnetic center and their signals appear at 10.90 ppm.[46] The peaks in the 6.90-8.10 ppm region most likely correspond to the rhodamine B moiety and traces of the free ligand [**4**]Cl (*see Supporting Information, Figure S3*). In the ESI-MS spectrum a peak at m/z=937.7 for $[\mathbf{5}]^+$, and at 902.5 for $[\mathbf{5}–Cl–H]^+$ were found that confirmed the formation of compound [**5**]Cl.

In the second step, the complex [Ru(**4**)(bpy)(Cl)]$(PF_6)_2$ ([**6**]$(PF_6)_2$) was obtained as a purple solid via treatment of [**5**]Cl with 2,2'-bipyridine in presence of EtN_3 and LiCl in an

ethanol/water mixture, followed by column chromatography and precipitation with aqueous KPF_6. Finally, the water soluble, potentially photosensitive ruthenium complex [Ru(**4**)(bpy)(Hmte)]Cl_3 ([**2**]Cl_3) was synthesized by removal of the chloride ligand in [**6**]$(PF_6)_2$ using $AgPF_6$ in presence of an excess of Hmte at elevated temperatures. The PF_6^- counter ions were then exchanged using a chloride-loaded exchange resin, to form the purple, water-soluble complex [**2**]Cl_3. ^{1}H NMR in methanol-d_4 showed that the protons of the coordinated Hmte ligand (3.46, 1.81, and 1.36 ppm) are shielded in [**2**]Cl_3 compared to free Hmte (3.75, 2.80, and 2.30 ppm). Moreover, the characteristic aromatic proton for [**2**]Cl_3 at 9.80 ppm (6A) appears at different chemical shift compared to that in [**6**]$(PF_6)_2$ (10.28 ppm). The high resolution mass spectrum showed two peaks for the product at m/z=360.45780 ([**2**]$^{3+}$) and at m/z=540.18289 ([**2**–H]$^{2+}$). Overall the analogous complexes [**2**]Cl_3 and [**1**]$(BF_4)_2$, which was synthesized as reported previously,[39] are soluble enough in water for studying their photophysical properties and the photosensitivity of their Ru-S bond.

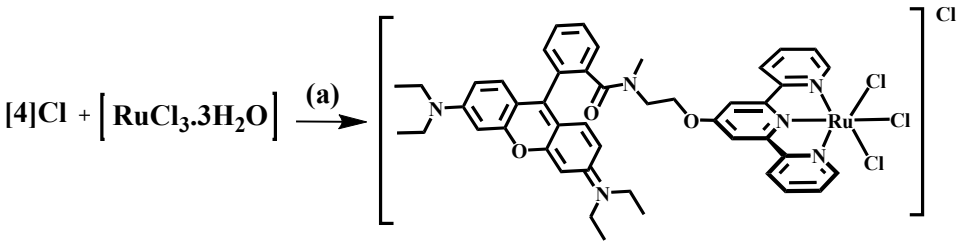

[**5**]Cl

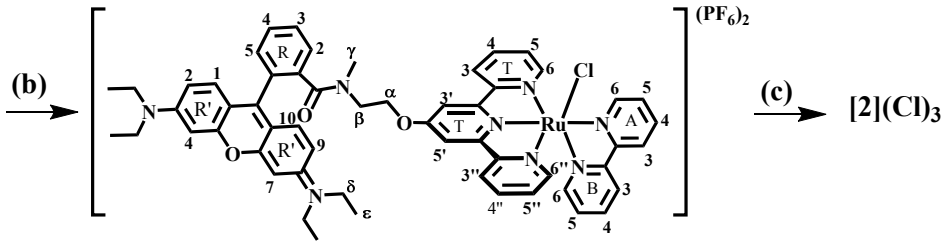

[**6**]$(PF_6)_2$

Scheme 2. Synthetic route towards ruthenium complexes [**5**]Cl, [**6**]$(PF_6)_2$, and [**2**]Cl_3. (a) MeOH, reflux, 7 h, yield: 54% (b) I: bpy, LiCl, NEt_3, EtOH/H_2O(3:1), reflux, 6 h. II: KPF_6 in water. Yield: 40% (c) I: Hmte, $AgPF_6$ (2.6 eq), acetone:H_2O (5:3), reflux, 9 h. II: chloride exchange DOWEX resin, acetone:H_2O (1:1), 4 h, r.t. Yield: 43%.

Emission measurements and energy transfer. As reported by Etchenique *et al.* for a similar rhodamine-ruthenium system,[38] the use of a short linker in $[\mathbf{2}]^{3+}$ was expected to allow at least some of the energy absorbed by rhodamine B to be donated to the ruthenium center in the covalent dyad. The emission and absorption spectra of $[\mathbf{2}]Cl_3$ were measured in water and compared to that of [**4**]Cl and rhodamine B (Figure 2b). All compounds absorb strongly in the yellow region, with extinction coefficient diminished in [**4**]Cl and $[\mathbf{2}]Cl_3$, however, compared to rhodamine (Table 1). In addition, the emission spectrum of the dyad $[\mathbf{2}]^{3+}$ shows almost complete quenching of the fluorescence of the rhodamine moiety upon excitation at 570 nm. This effect is not observed with ligand $[\mathbf{4}]^{+}$, which keeps a significant part of the rhodamine fluorescence, characterized by an emission quantum yield φ_4 of 0.12(2) (see Figure 2b and Experimental Part). In the dyad $[\mathbf{2}]^{3+}$ the overlap integral between the emission spectrum of the rhodamine fragment (modeled as $[\mathbf{4}]^{+}$) and the absorbance spectrum of the ruthenium moiety (modeled as $[\mathbf{1}]^{2+}$) was calculated, from which a Förster distance R_0=20.5 Å was found (see Experimental Part and Figure S10). In classical photophysics R_0 represents the distance at which Förster Resonance Energy Transfer (FRET) occurs with an efficiency of 50% (see Experimental Part and Supplementary Information). To evaluate the typical intramolecular distance between the rhodamine fragment and the ruthenium moiety in $[\mathbf{2}]^{3+}$ a theoretical model of the dyad was prepared in an extended conformation, and minimized by DFT (see Experimental Part). In the minimized structure the distance between the centroid of the central aromatic ring of rhodamine, and the nitrogen atom of the central pyridine ring of the terpyridine ligand, was found to be r=12.1 Å. This distance is ~1.7 shorter than R_0, which predicts efficient to very efficient (φ_{FRET} ~ 96%) FRET to occur from the rhodamine dye to the ruthenium fragment of $[\mathbf{2}]^{3+}$ upon irradiation at 570 nm. In absence of additional non-radiative decay, such energy transfer might lead to photosubstitution of the Hmte ligand.

Table 1. Spectroscopic data in MilliQ water for compounds [**2**]Cl_3, [**4**]Cl, and rhodamine B. Emission data were obtained upon excitation at λ=570 nm.

Compound	$\varepsilon_{(\lambda Max)}$ ($M^{-1}.cm^{-1}$)	λ_{max} (abs) (nm)	λ_{max} (em) (nm)
rhodamine B	120000	555	576
[**4**]Cl	74000	569	586
[**2**]Cl_3	44000	570	585

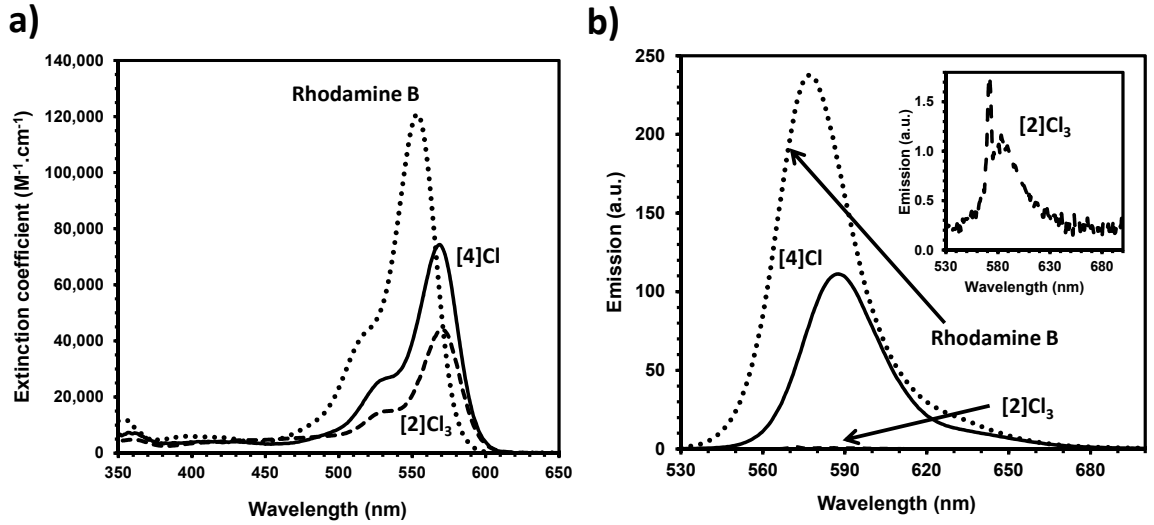

Figure 2. Absorption (a) and emission (b) spectra of rhodamine B, rhodamine B-terpyridine conjugate [**4**]Cl, and rhodamine B-functionalized ruthenium complex [**2**]Cl_3 in MilliQ water at *pH*=7. Excitation: 570 nm, slit width: 3 nm. The concentrations of the solutions used for emission measurements were taken such that their absorbance at 570 nm were identical in the three solutions (A_{570}=0.23).

Photochemistry. In order to check whether emission quenching of the rhodamine fragment in $[\mathbf{2}]^{3+}$ was indeed due to energy transfer to ruthenium the photoreactivity of the dyad [**2**]Cl_3 was investigated upon yellow and blue light irradiation. Irradiation with blue light, *i.e.*, in the ^{1}MLCT band of the ruthenium complex, is expected to lead to the photosubstitution of the Hmte ligand by an aqua ligand, to form $[Ru(\mathbf{4})(bpy)(OH_2)]^{2+}$ (complex $[\mathbf{7}]^{3+}$, see Scheme 3). The formation of $[\mathbf{7}]^{3+}$ was first monitored by ^{1}H NMR spectroscopy in D_2O. NMR samples containing [**2**]Cl_3 in degassed D_2O were prepared, and the samples were irradiated with blue

(λ_e = 452 nm) or yellow light (λ_e = 570 nm) at room temperature. While the ^{1}H NMR spectrum of a reference sample in the dark did not change, the spectra of the irradiated samples showed the gradual disappearance of the starting compound $[\mathbf{2}]^{3+}$ (δ=9.76 ppm for proton 6A, and δ=3.48 ppm, 1.83 ppm, and 1.37 ppm for coordinated Hmte) and the formation of a single new ruthenium complex (δ=9.61 ppm for proton 6A) and of the free Hmte ligand (at δ=3.74, 2.66, and 2.01 ppm). Figure 3 shows the evolution of the ^{1}H NMR spectra for proton 6A upon irradiation (the complete spectra before and after irradiation are shown in Figure S6). Mass spectra after irradiation were obtained for both samples, and the peak found at 339.6 is characteristic for the formation of $[Ru(\mathbf{4})(bpy)(D_2O)]^{3+}$. Integration of the protons 6A for $[\mathbf{2}]^{3+}$ and $[\mathbf{7}]^{3+}$ indicated typically 40% photoconversion of $[\mathbf{2}]^{3+}$ to $[\mathbf{7}]^{3+}$ after about 500 min irradiation. The present data show that a substantial amount of Hmte is indeed photosubstituted, not only upon blue light irradiation but also upon yellow light irradiation, which is absorbed by the rhodamine dye more than by the ruthenium fragment (see below). However, these NMR experiments could not provide quantitative information on the quantum efficiency of the light-induced substitution reaction, as light intensities in the irradiation setup were difficult to determine.

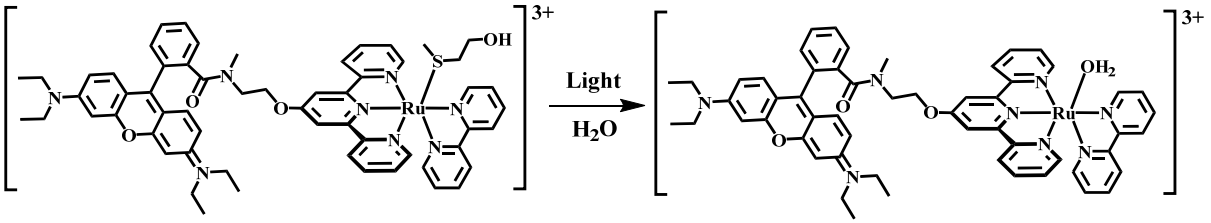

$[\mathbf{2}]^{3+}$ $[\mathbf{7}]^{3+}$

Scheme 3. Photosubstitution of Hmte in $[\mathbf{2}]^{3+}$ by an aqua ligand to form $[\mathbf{7}]^{3+}$ upon blue light (λ_e=452 nm) or yellow light (λ_e=570 nm) irradiation in aqueous solution.

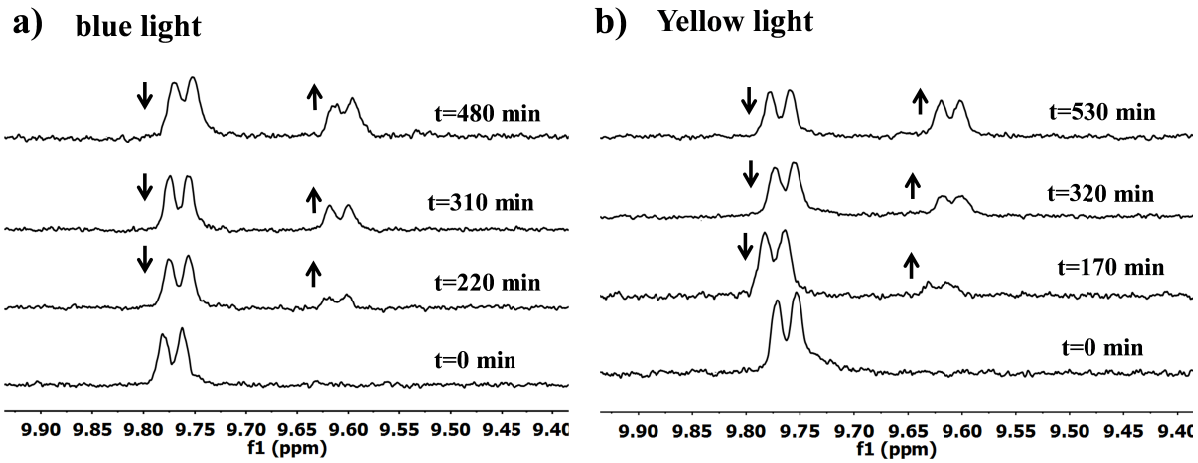

Figure 3. Evolution of the ^{1}H NMR spectra of degassed D_2O solution of [**2**]Cl_3 upon irradiation with a) blue light (λ_e=452 nm, $\Delta\lambda_{1/2}$=8.9 nm) or b) yellow light (λ_e=570 nm, $\Delta\lambda_{1/2}$=8.9 nm). Irradiation times are indicated for each spectrum. Conditions: total ruthenium concentration $[Ru]_{tot}=5.3\times10^{-3}$ M, room temperature.

In order to get quantitative information about the yellow and blue light-triggered release of Hmte from complex [**2**]$^{3+}$, UV-vis experiments were performed in well-controlled irradiation conditions. An aqueous solution of [**2**]Cl_3 was exposed to yellow light (570 nm) or blue light (452 nm) shining light from the top of a UV-vis cuvette placed inside the spectrophotometer (see Supplementary Information). The UV-vis spectra were measured perpendicular to the irradiating light beam, during light irradiation. As shown in Figure 4a, the absorption spectrum of complex [**2**]$^{3+}$ gradually evolved until a steady state was obtained after 150 and 320 mintues of irradiation with yellow and blue light, respectively. Isosbestic points at 380 nm, 460 nm, and 557 nm indicate the occurance of only one photochemical reaction. From the ^{1}H NMR and mass spectrometry studies it is clear that extensive irradiation of [**2**]$^{3+}$ leads to the full photoconversion into the aqua complex [**7**]$^{3+}$ ($RuOH_2$) (see *Supporting Information, Figure S7*). Thus, in each experiment the concentration of [**2**]$^{3+}$ and [**7**]$^{3+}$ could be calculated from the extinction coefficients of both species (*see Supporting Information*). Using Equation 1, the photochemical substitution first-order rate constants $k_{\varphi570}$ and $k_{\varphi452}$ could be obtained from the slope of a plot of ln($[RuHmte]/[Ru]_{tot}$) *vs.* irradiation time (Figure

5a, I-II), where *[RuHmte]* and $[Ru]_{tot}$ represent the concentration in $[\mathbf{2}]^{3+}$ and the total ruthenium concentration in the solution, respectively. Half-reaction times were calculated using Equation 2. The data are reported in Table 2; they show that the photoconversion rate upon yellow light irradiation, $k_{\varphi 570}$, was twice higher compared to that obtained upon blue light irradiation ($k_{\varphi 452}$). Since the photon flux values at 570 nm and 452 nm (Φ_{570} and Φ_{452}) were not equal, the rate constants $k_{\varphi 570}$ and $k_{\varphi 452}$ cannot be directly compared, but the photosubstitution quantum yields have to be calculated instead. As expressed in Equation 3, the photosubstitution rate constant depends on the photon flux Φ, the extinction coefficient $\varepsilon_{\lambda e}$ of RuHmte at the irradiation wavelength, the total absorbance at the irradiation wavelength A_e, the probability of absorbance of the photon $(1-10^{-Ae})$, the photosubstitution quantum yield φ, the irradiation pathlength L, and the irradiated volume V.

$$-\frac{dn_{RuHmte}}{dt} = \frac{dn_{RuOH_2}}{dt} = k_{\varphi}.n_{RuHmte} \quad \text{(Equation 1)}$$

$$t_{1/2} = \frac{ln2}{k_{\varphi}} \quad \text{(Equation 2)}$$

$$k_{\varphi} = \Phi \cdot (1 - 10^{-A_e}) \cdot \left(\frac{\varepsilon_{\lambda_e}.L}{A_e.V}\right) \cdot \varphi \quad \text{(Equation 3)}$$

The number of moles of RuHmte remaining in solution, n_{RuHmte}, was plotted *vs.* the number of moles of photons Q absorbed at time t since t=0, by RuHmte (Figure 5b and *Supporting Information*). The photosubstitution quantum yields were obtained directly from the slope of these plots; they were found to be $8.5(6)\times10^{-3}$ and $9.2(7)\times10^{-3}$ for yellow and blue light irradiation, respectively (Table 2). These values are similar, which demonstrates that once absorbed a yellow photon has almost the same probability to lead to ligand photosubstitution as a blue photon. This can be considered as a generalization of Kasha's rule, which states that the emission quantum yield of a fluorophore is independent from the excitation wavelength.

However, the quantity of $RuOH_2$ formed in a given irradiation time depends on the amount of light absorbed by the complex at the irradiation wavelength as well. In this regard, the extinction coefficients of compound $[\mathbf{2}]^{3+}$ at 570 nm and 452 nm are very different ($4.4(2)\times10^4$ and $4.8(2)\times10^3$, respectively). Thus, in order to compare the photosubstitution rates the extinction coefficients must be considered as well. Multiplying the extinction coefficient by the photosubstitution quantum yield gives a value called the photosubstitution reactivity (ξ),[38] which best represents how fast a photoreaction will occur under a given photon flux. Actually, Equation 3 simplifies into Equation 4 when the absorbance A_e is small compared to 1:

$$k_\varphi \approx \left(ln\,10 \cdot \frac{L}{V}\right) \cdot \Phi \cdot \varepsilon_{\lambda_e} \cdot \varphi = \left(ln\,10 \cdot \frac{L}{V}\right) \cdot \Phi \cdot \xi \quad \text{(Equation 4)}$$

The calculated values of ξ are reported in Table 2. These values show that for complex $[\mathbf{2}]^{3+}$ Hmte substitution is one order of magnitude faster with yellow light than with blue light. In fact, ten times more moles of photoproduct ($[\mathbf{7}]^{3+}$) were produced upon yellow light irradiation compared to blue light irradiation at short reaction times. Quantitatively, the higher molar absorptivity at 570 nm of complex $[\mathbf{2}]^{3+}$ due to the allowed character of the intraligand π-π* transition of the rhodamine B moiety, promotes intensive absorption of yellow photons compared to blue ones.

In order to evaluate the influence of the rhodamine B antenna on the photosubstitution of Hmte, similar irradiation experiments were performed on its analogue complex $[\mathbf{1}]^{2+}$, which does not have the fluorophore antenna. Upon yellow light irradiation (570 nm) the absorption band of $[\mathbf{1}]^{2+}$ at 450 nm gradually disappeared to give rise to a new absorption maximum at higher wavelength corresponding to $[Ru(terpy)(bpy)(OH_2)]^{2+}$ ($[\mathbf{8}]^{2+}$, see Figure 4b). The first-order photosubstitution rate constant was obtained from the slope of the plots of $\ln([RuHmte]/[Ru]_{tot})$ *vs.* irradiation time (Figure 5a, III), and the photosubstitution quantum yield was obtained as described above (Figure 5b, III). The photosubstitution quantum yield

of compound $[\mathbf{1}]^{2+}$ upon blue light irradiation was recently published by our group using different irradiation conditions.[39] For better comparison with $[\mathbf{2}]^{3+}$ we repeated the measurement in the same irradiation conditions as for $[\mathbf{2}]^{3+}$ (Figure 5, IV). All photochemical data, including half-reaction times, are reported in Table 2. Like for $[\mathbf{2}]^{3+}$ the photosubstitution quantum yields for $[\mathbf{1}]^{2+}$ upon blue light and yellow light irradiations were found very close to each other, *i.e.*, 0.016(4) *vs.* 0.011(4), respectively. This result confirms our observations on $[\mathbf{2}]^{3+}$, that once absorbed by $[\mathbf{1}]^{2+}$ yellow photons are able to lead to ligand photosubstitution as efficiently as blue photons.

In order to compare the photoreactivity of different compounds one should compare their ξ values, which depends on both the extinction coefficient (ε_λ) and the photosubstitution quantum yield (φ_λ). Although the photosubstitution quantum yields at 570 nm and 452 nm are comparable for both complexes $[\mathbf{1}]^{2+}$ and $[\mathbf{2}]^{3+}$, the extinction coefficient at 570 nm (ε_{570}) is two order of magnitudes higher for $[\mathbf{2}]^{3+}$ than for $[\mathbf{1}]^{2+}$ due to the presence of the yellow-absorbing dye, while the values of ε_{452} are of the same order of magnitude for both complexes. As a result, under yellow light irradiation ξ is about two orders of magnitude higher for $[\mathbf{2}]^{3+}$ than for $[\mathbf{1}]^{2+}$, and it is still four times higher than that of $[\mathbf{1}]^{2+}$ under blue light irradiation. Overall, at constant photon flux it is the different extinction coefficients (ε_λ) that mostly influences the photosubstitution rate constants for $[\mathbf{1}]^{2+}$ and $[\mathbf{2}]^{3+}$ at 450 or 570 nm, whereas their quantum yields poorly depend on irradiation wavelength.

This result is similar to Kasha's rule, which states that the fluorescence quantum yield of a fluorophore is independent on the irradiation wavelength.[47] Indeed, like for fluorophores where emission always occurs from the lowest singlet excited state, for ruthenium complexes such as $[\mathbf{1}]^{2+}$ or $[\mathbf{2}]^{3+}$ photosubstitution is expected to occur from a ruthenium-based ^{3}MLCT state *via* thermal promotion to a nearby dissociative ^{3}MC state. Reaching the ^{3}MLCT state can be done either by direct excitation of the ^{1}MLCT band of the ruthenium complex, or by

excitation of the rhodamine dye followed by energy transfer to the ruthenium fragment. In the case of a direct excitation of the metal complex ($[\mathbf{1}]^{2+}$) yellow photons need to be absorbed by vibrationally excited ground-state complexes, to be able to lead to the ^{3}MLCT excited state. Once there, non-radiative decay will occur with almost the same probability as when the ^{3}MLCT state is obtained by absorption of a blue photons by a non-vibrationally excited ground state complex. In the case of indirect excitation of $[\mathbf{2}]^{3+}$ with yellow photon the ^{3}MLCT state is probably reached efficiently *via* absorption by the rhodamine group, followed by energy transfer. While from Etchenique's work energy transfer was expected to occur in $[\mathbf{2}]^{3+}$, it was not expected to be *that* efficient.

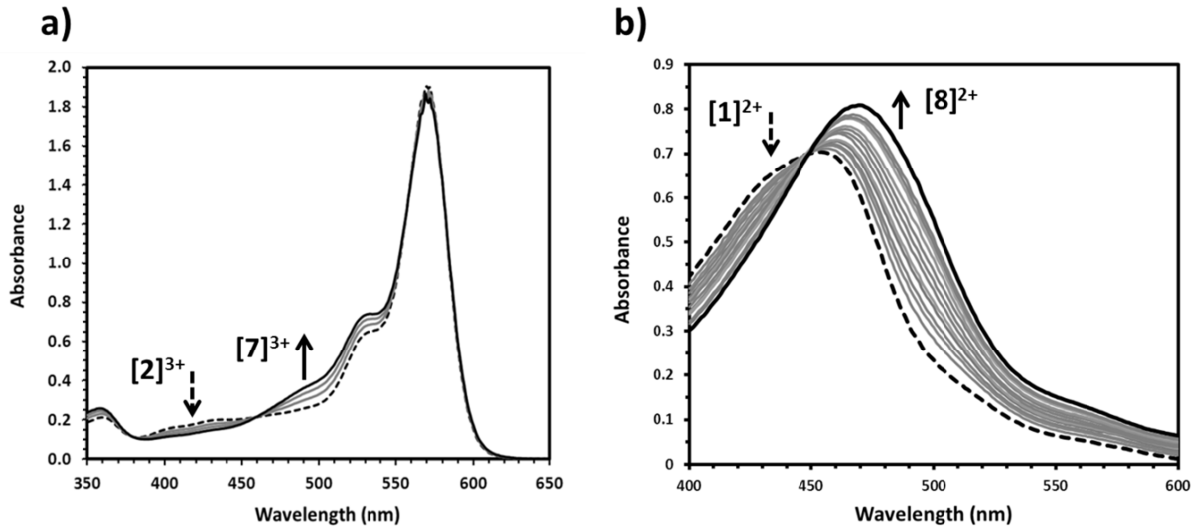

Figure 4. a) Time evolution of the UV-vis spectrum of an aqueous solution of a) $[\mathbf{2}]^{3+}$ and b) $[\mathbf{1}]^{2+}$ irradiated with yellow light (λ_e=570 nm). Condition: photon flux Φ=5.3×10^{-9} Einstein.s^{-1}, irradiation pathlength=3 cm, T=298 K. Total ruthenium concentrations: a) $[Ru]_{tot}$ =3.4×10^{-5} M b) $[Ru]_{tot}$ =1.2×10^{-4} M.

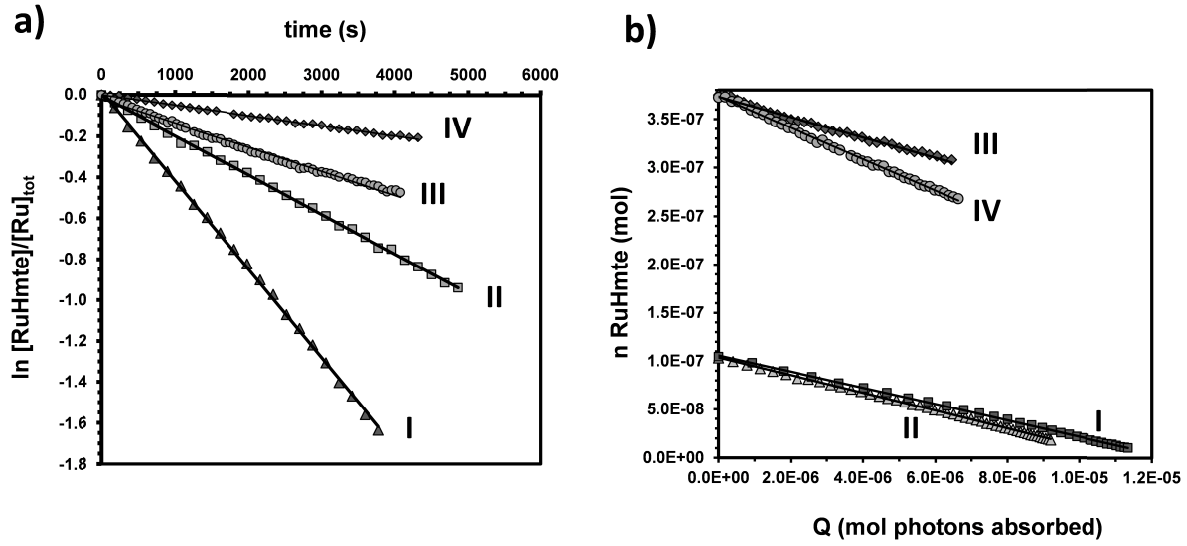

Figure 5. a) Plots of *ln([RuHmte]/[Ru]$_{tot}$) vs.* irradiation time; *[RuHmte]* represents the concentration in $[\mathbf{2}]^{3+}$ or $[\mathbf{1}]^{2+}$, and *[Ru]$_{tot}$* the total ruthenium concentration in the solution. The slope of each plot is k_φ (s^{-1}). b) Plots of the number of moles of RuHmte *vs.* the number of moles of photons absorbed by RuHmte at time t, since t=0; the slope is the photosubstitution quantum yield φ. I) RuHmte=$[\mathbf{2}]^{3+}$, *[Ru]$_{tot}$*=3.4×10^{-5} M, yellow light (λ_e=570 nm). II) RuHmte=$[\mathbf{2}]^{3+}$, *[Ru]$_{tot}$*=3.4×10^{-5} M, blue light (λ_e=452 nm). III) RuHmte=$[\mathbf{1}]^{2+}$, *[Ru]$_{tot}$*=1.2×10^{-4} M, yellow light (λ_e=570 nm). IV) RuHmte=$[\mathbf{1}]^{2+}$, *[Ru]$_{tot}$*=1.2×10^{-4} M, blue light (λ_e=452 nm). Photon fluxes: Φ_{570}=$5.3(8)\times10^{-9}$ Einstein.s^{-1} and Φ_{452}=$3.0(6)\times10^{-9}$ Einstein.s^{-1}.

Table 2. Photochemical data for the photosubstitution of Hmte by H_2O in $[\mathbf{2}]^{3+}$ and $[\mathbf{1}]^{2+}$ in MilliQ water. Condition: T=298 K, irradiation pathlength=3 cm, concentration in $[\mathbf{2}]^{3+}$: 3.4×10^{-5} M, concentration in $[\mathbf{1}]^{2+}$: 1.2×10^{-4} M.

Ru complex	λ_e (nm)	$\varepsilon_{\lambda e}$ ($M^{-1}.cm^{-1}$)	Φ (Einstein.s^{-1})	k_φ (s^{-1})	$t_{(1/2)}$ (min)	φ	ξ ($\varphi\times\varepsilon_{\lambda e}$)
$[\mathbf{2}]^{3+}$	570	44000	$5.3(8)\times10^{-9}$	$4.4(3)\times10^{-4}$	26(2)	$8.5(6)\times10^{-3}$	370(15)
$[\mathbf{2}]^{3+}$	452	4800	$3.0(6)\times10^{-9}$	$1.9(3)\times10^{-4}$	59(2)	$9.2(7)\times10^{-3}$	44(8)
$[\mathbf{1}]^{2+}$	570	450	$5.3(8)\times10^{-9}$	$5.2(2)\times10^{-5}$	220(5)	$1.1(4)\times10^{-2}$	4.8(5)
$[\mathbf{1}]^{2+}$	452	6600	$3.0(6)\times10^{-9}$	$1.3(4)\times10^{-4}$	89(3)	$1.6(4)\times10^{-2}$	100(10)

Discussion

The covalent binding of a rhodamine B dye to the terpy ligand of the ruthenium complex in $[\mathbf{2}]^{3+}$ leads to rather efficient photosensitization, as photosubstitution upon yellow light irradiation became faster even compared to blue light irradiation of the parent complex $[\mathbf{1}]^{2+}$. Sensitization seems to occur *via* energy transfer from the rhodamine B sensitizer to the ruthenium complex, as reported by Etchenique.[38] By using a short saturated linker, the attachment of rhodamine B to the ruthenium complex occurs without mixing the orbitals of the dye and that of the ruthenium complex. Thus, we assume that the spectrum of $[\mathbf{1}]^{2+}$ is a good model for the contribution of the ruthenium moiety to the spectrum of $[\mathbf{2}]^{3+}$, *i.e.*, that the excited states of the rhodamine B part and of the ruthenium part in $[\mathbf{2}]^{3+}$ are not too much affected by each other. By comparing the extinction coefficient of $[\mathbf{2}]^{3+}$ with that of $[\mathbf{1}]^{2+}$ in Table 2, it appears that only 1% of the yellow photons are absorbed by the ruthenium-centered ^{1}MLCT band in $[\mathbf{2}]^{3+}$, while this fraction goes up to 73% for blue photons. In fact, the presence of rhodamine B is not significantly interfering with the MLCT-based blue photon absorption in $[\mathbf{2}]^{3+}$, whereas, it contributes largely to yellow photon absorption.

Considering on the one hand the almost full fluorescence quenching of the rhodamine B moiety in $[\mathbf{2}]^{3+}$, and on the other hand the very similar photosubstitution quantum yields upon blue (direct) and yellow (indirect) light irradiation, energy transfer from the rhodamine B moiety to the ruthenium center appears to be highly efficient in $[\mathbf{2}]^{3+}$. Thus, non-radiative decay probably occurs mostly from the ^{3}MLCT state of the ruthenium moiety, rather than from the S1 excited state of the rhodamine B moiety. Although deeper photophysical studies would be needed to assess the exact nature of the energy transfer mechanism, according to Etchenique's work and to the low r/R_0 ratio (see above) the energy transfer in $[\mathbf{2}]^{3+}$ is expected to occur *via* reverse Förster Resonance Energy Transfer (reverse FRET), *i.e.*, the modest spectral overlap between the emission of the FRET donor and the absorption of the

ruthenium acceptor is compensated by the very short distance between both components in the dyad. Other types of energy transfer mechanisms, such as Dexter's,[32] would require direct orbital overlap between the donor and the acceptor, which, considering the saturated nature of the linker and the similar shapes of the absorption spectrum of [**2**]Cl_3 and of [**4**]Cl, seems very unlikely.

From a pure photochemical point of view, the sensitization of photosusbtitution reactions might find application in photoactivated chemotherapy (PACT), for which the practical efficiency of a given compound will depend on the amount of photoproduct generated in a given irradiation time. Thus, at a given light intensity the photosubstitution quantum yield does not matter too much, but it is the photosubstitution reactivity ξ, which also takes the extinction coefficient into account, that should be considered. On the other hand, it cannot be forgotten that functionalization of a light-activatable metallodrug with large, flat aromatic dye is expected to change many biological properties of the complex such as its lipophilicity, uptake mechanism, and/or mechanism of cytotoxicity. In the end, only compounds that combine good uptake, a low toxicity in the dark, a high toxicity after ligand substitution, *and* a high photosubstitution reactivity, might be interesting for medicinal purposes.

Conclusions

Our data show that yellow photons that do not seem to have enough energy to populate the ^{1}MLCT state of [**1**]$^{2+}$ or [**2**]$^{3+}$ lead, once absorbed, to photosubstitution of Hmte with almost the same quantum efficiency as that achieved with blue photons. Thus, for this family of ruthenium compounds Kasha's rule remains valid, *i.e.*, the quantum efficiency of photosubstitution reactions does not depend on the energy of the incoming photons. However, for practical applications irradiating photosensitive complexes such as [**1**]$^{2+}$ far down their absorption band does render photon collection less efficient. Upon covalent

attachment of an organic dye with high molar absorptivity (here rhodamine B for yellow photons) the photon collection problem was solved, and for complex $[\mathbf{2}]^{3+}$ efficient energy transfer from the dye to the ruthenium center was observed. The resulting photosubstitution reactivity under yellow light irradiation became even higher than that of compound $[\mathbf{1}]^{2+}$ under blue light irradiation, due to the much improved collection of yellow photons.

To conclude, it may be noted that sensitizing the ruthenium complex with dyes absorbing at still higher wavelengths, *i.e.*, up in the red region, might become increasingly difficult. The efficiency of energy transfer is expected to decrease when the spectrum overlap between the emission of the dye and the MLCT band of the ruthenium complex becomes smaller, as a result of which sensitization might not remain possible with dyes that absorb too far in the red region. In the extreme case of negligible spectral overlap, the photoreactivity of the metal center and the emission of the fluorophore are expected to decouple. In such a case, the absorbed photons would lead either to ligand photosubstitution, or to fluorescence, depending on the irradiation wavelength. Such systems might find potential application in molecular imaging, for example to probe the position of a ruthenium complex and follow its fate, either in biological or in artificial systems. [18, 48]

Experimental Section

General. ^{1}H and ^{13}C NMR spectra were recorded using a Bruker DPX-300 spectrometer; chemical shifts are indicated in ppm relative to TMS. Electrospray mass spectra were recorded on a Finnigan TSQ-quantum instrument by using an electrospray ionization technique (ESI-MS). High resolution mass spectrometry was performed using a Thermo Finnigan LTQ Orbitrap mass spectrometer equipped with an electrospray ion source (ESI) in positive mode (source voltage 3.5 kV, sheath gas flow 10, capillary temperature 275 ºC) with resolution R = 60.000 at m/z = 400 (mass range = 150-200) and dioctylphtalate (m/z =

391.28428) as "lock mass". UV-vis spectra were obtained on a Varian Cary 50 UV-vis spectrometer. Emission spectra were obtained using Shimadzu RF-5301 spectrofluorimeter. The irradiation setup was a LOT 1000 W Xenon arc lamp, fitted with a 400FH90-50 Andover standard cutoff filter and a Andover 450FS10-50 (λ_e=452 nm, $\Delta\lambda_{1/2}$=8.9 nm) or a 570FS10-50 (λ_e=570 nm, $\Delta\lambda_{1/2}$=8.9 nm) interference filter. DMSO and dichloroethane were dried over $CaSO_4$ and distilled before use. CH_3CN was dried using a solvent dispenser PureSolve 400. 4'-Chloro-2,2':6',2''-terpyridine[49] and [Ru(terpy)(bpy)(Hmte)]$(BF_4)_2$ ([**1**]$(BF_4)_2$[39] were synthesized following literature procedures. $AgPF_6$, LiCl, KPF_6 and the anionic exchange resin DOWEX 22 were purchased from Sigma-Aldrich. Triethylamine was purchased from Acros; KOH and $POCl_3$ were purchased from Merck; and rhodamine B was purchased from Lambda Physik. The eluent for column chromatography purification of compound [**6**]$(PF_6)_2$ was prepared by mixing MeCN, MeOH, and H_2O 66:17:17 ratio, followed by addition of solid NaCl until saturation was reached.

Synthesis

Compound 3. 2-methylaminoethanol (45 mg, 0.60 mmol) was added to a suspension of powdered KOH (94 mg, 1.7 mmol) in dry DMSO (2 mL). The mixture was stirred for 30 min at 60 ºC. 4'-chloro-2,2':6',2''-terpyridine (160 mg, 0.600 mmol) was added and the mixture was stirred at 60 ºC for 3 h and then overnight at r.t. Then, the mixture was poured onto water (60 mL). The aqueous phase was extracted with DCM (3×30 mL) and the organic phases were combined and dried over $MgSO_4$. DCM was evaporated under reduced pressure and the product was left 24 h under high vacuum at 40 ºC to remove trace amounts of DMSO. Compound **3** was obtained as pale yellow oil (160 mg, 0.520 mmol, 87% yield). ^{1}H NMR (300 MHz, CD_3OD, 298 K, *see Figure S1 for proton attribution*) δ (ppm) 8.61 (d, J = 4.8 Hz, 2H, T66''), 8.54 (d, J = 8.0 Hz, 2H, T33''), 7.96 – 7.87 (m, 4H, T44''+ T3' + T5'), 7.41

(ddd, J = 7.5, 4.8, 1.1 Hz, 2H, T44''), 4.29 (t, J = 5.2 Hz, 2H, α), 3.00 (t, J = 5.2 Hz, 2H, β), 2.46 (s, 3H, γ). ^{13}C NMR (75 MHz, CD_3OD, 298 K) δ (ppm) 168.39 (T4'), 158.32 (T1), 157.03 (T1'), 150.09 (T66''), 138.68 (T3',T5'), 125.43 (T44''), 122.91 (T33''), 108.35 (T44''), 68.18 (α), 50.84 (β), 35.85 (γ). High resolution ES-MS m/z (calc): 307.15589 (307.15516, $[M+H]^+$).

Compound [4]Cl. Following a literature procedure[43] phosphorus oxychloride (60.0 μL, 0.657 mmol) was added to a solution of rhodamine B (150 mg, 0.313 mmol) in dry 1,2-dichloroethane (5 mL). The mixture was refluxed for 5 h. The solvent was evaporated under reduced pressure and the crude mixture was immediately re-dissolved in dry CH_3CN (10 mL). Et_3N (131 μL, 0.939 mmol) and compound **3** (96 mg, 0.31 mmol) were added and the mixture was refluxed for 14 h. The solvent was evaporated under reduced pressure at 30 ºC and the crude product was dissolved in water and filtered to remove any solid. The product was precipitated by addition of KPF_6, filtered, washed with H_2O, and dried in a desiccator at ambient pressure over silica gel blue for 4 h. Exchange of the PF_6^- counter anions with Cl^- was achieved by stirring an acetone/water solution (1:1) of the product with the Cl^- exchange resin DOWEX 22 (2.0 g) for 4 h. The resin was filtered, acetone was evaporated under reduced pressure at 22 ºC, and water was removed using a freeze drier. The product was purified by column chromatography on silica gel ($CHCl_3$/MeOH, 10% to 20% of MeOH). Solvents were evaporated under reduced pressure and compound [**4**]Cl was obtained as a purple solid (75 mg, 0.097 mmol, 31%). ^{1}H NMR (300 MHz, CD_3OD, 298 K, *see Figure S2 for proton attribution*) δ (ppm) 8.77 – 8.70 (m, 4H, T33'', T66''), 8.06 (td, J = 7.7, 1.8 Hz, 2H, T44''), 7.84 – 7.72 (m, 3H,5R,4R,3R), 7.70 (s, 2H, T3',T5'), 7.54 (ddd, J = 7.5, 4.8, 1.2 Hz, 2H, T44''), 7.47 (dd, J = 6.5, 1.0 Hz, 1H, 5R), 7.34 (d, J = 9.6 Hz, 2H, 10R',1R'), 7.01 (dd, J = 9.6, 2.5 Hz, 2H, 2R',9R'), 6.44 (d, J = 2.4 Hz, 2H, 4R',7R'), 3.84 (t, J = 4.3 Hz, 2H, α), 3.74 (t, J = 4.3 Hz, 2H, β), 3.41 (dd, J = 13.4, 6.6 Hz, 8H, δ), 2.96 (s, 3H, γ), 1.14 (t, J =

7.1 Hz, 12H, ε). ^{13}C NMR (75 MHz, CD_3OD, 298 K) δ (ppm) 171.10 (C=O), 167.99 (3R,8R), 158.80, 158.25, 157.00, 156.87, 156.30, 150.30 (T66''), 138.82 (T55''), 137.59, 133.31 (2R'+9R'), 131.73+131.65 (3R+2R+4R), 131.17, 130.99 (5R), 128.75 (T5'), 125.78 (T44''), 122.89 (T33''), 115.19 (1R'+10R'), 114.43, 108.06 (T'3), 97.19 (4R'+7R'), 68.13 (α+β), 46.80 (δ), 40.53 (γ), 12.78 (ε). High resolution ES-MS m/z (calc): 731.37096 (731.37041 $[M]^+$). UV-vis: λ_{max} (ε in $L \cdot mol^{-1} \cdot cm^{-1}$) in pure H_2O: 569 nm (74000). Anal. Calcd for $C_{46}H_{47}ClN_6O_3 \cdot CHCl_3 \cdot H_2O$: C, 62.39; H, 5.57; N, 9.29. Found: C, 61.77; H, 5.75; N, 9.68.

Compound [5]Cl. Compound [**4**]Cl (120 mg, 0.156 mmol) and $RuCl_3 \cdot 3H_2O$ (41 mg, 0.16 mmol) were dissolved in MeOH (20 mL) and refluxed for 7 h under argon. The mixture was first cooled down to room temperature, and then cooled in an ice bath for 30 min and overnight in the fridge. The precipitate was filtered off and air dried to yield [**5**]Cl as a dark purple powder (83 mg, 0.075 mmol, 54%). ^{1}H NMR (300 MHz, CD3OD, 298 K, *see Figure S3 for proton attribution*) δ (ppm) 10.90 (s, T3',T5'), 8.07 – 7.88 (m, 3H), 7.69 (d, J = 6.9 Hz, 2H), 7.55 (d, J = 9.4 Hz, 2H), 7.01 (d, J = 9.7 Hz, 3H), −1.43 (s, T33''/T44''/T55''), −10.26 (s, T33''/T44''/T55''), −10.71 (s, T33''/T44''/T55''), −35.94 (s, T66''). ES-MS m/z (calc): 938.2 (937.7 $[M-Cl]^+$), 902.2 (902.5 $[M-2Cl-H]^+$).

Compound [6](PF$_6$)$_2$. [**5**]Cl (78 mg, 0.080 mmol), 2,2'-bipyridine (13 mg, 0.083 mmol), and LiCl (5.0 mg, 0.12 mmol) were mixed in a 3:1 EtOH/H_2O mixture (15 mL) and the solution was degassed with argon for 5 min, after which Et_3N (15 μL, 0.10 mmol) was added. The reaction mixture was refluxed under argon for 6 h, and then it was filtered hot over celite. The filtrate was evaporated under reduced pressure. Column chromatography purification was performed over silica gel (eluent: MeCN / MeOH / H_2O, 66:17:17: saturated in NaCl, R_f=0.5). The solvent was evaporated, then the crude product was dissolved in water (50 mL), and precipitated by adding KPF_6 (~1 g). After filtration, washing with water and drying in a

desiccator at ambient pressure over silica gel blue for 5 h compound [**6**]$(PF_6)_2$ was obtained in 40% yield as a dark purple powder (41 mg, 0.031 mmol). ^{1}H NMR (300 MHz, CD_3OD, 298 K, *see Figure S4 for proton notation*) δ (ppm) 10.28 (d, J = 5.6 Hz, 1H, 6A), 8.79 (d, J = 8.2 Hz, 1H, 3A), 8.51 (d, J = 8.1 Hz, 3H, 10R' + 1R'+ 3B), 8.32 (t, J = 8.1 Hz, 1H, 4A), 8.07 – 7.91 (m, 5H, 2R'+ 9R'+ 7R'+ 5R+ 5A), 7.89 – 7.68 (m, 6H, T3'+ T5'+ 3R + 4B + T33''), 7.47 (d, J = 7.6 Hz, 1H, 2R), 7.44 – 7.31 (m, 5H, 4R'+ 4R + 5B+ T44''), 7.13 – 7.01 (m, 3H, 6B + T55''), 6.71 (d, J = 2.4 Hz, 2H, T66''), 4.02 (t, J = 4.5 Hz, 2H, α), 3.88 (d, J = 4.5 Hz, 2H, β), 3.45 (m, 8H, δ), 3.05 (s, 3H, γ), 1.31 (t, J = 12.9 Hz, 12H, *ε*). ^{13}C NMR (75 MHz, CD_3OD, 298 K) δ (ppm) ^{13}C NMR (75 MHz, CD_3OD, 298 K) δ 171.25 (C=O), 166.26 (3R,8R), 160.55, 160.48, 159.89, 159.07, 159.03, 158.19, 157.10, 153.86 (6A), 153.78, 152.85 (4R'), 138.42 (4R'+ 5R), 137.72 (4A), 137.64, 136.70 (T33''), 133.46 (T44''), 132.43 (2R), 131.99 (T3'), 131.89 (T5'), 130.98 (4B), 129.85 (3R), 128.74 (4R), 128.57 (5B), 127.96 (5A), 127.43 (6B), 125.09 (10R'+1R), 124.85 (3B), 124.58 (3A), 115.40 (T55''), 114.40, 110.89 (2R'+ 9R'), 97.76 (6T +6''T), 69.91(α+ β), 48.15 (δ) , 46.98 (γ), 13.04 (*ε*). High resolution ESI-MS m/z (calc): 512.15646 (512.15650 $[M-2PF_6]^{2+}$). UV-vis: λ_{max} (*ε* in $L \cdot mol^{-1} \cdot cm^{-1}$) in 9:1 acetone/$H_2O$:570 nm ($58 \times 10^3$).

Compound [2]Cl_3. [**6**]$(PF_6)_2$ (30 mg, 0.023 mmol) and $AgPF_6$ (15 mg, 0.060 mmol) were dissolved in a 3:5 acetone/H_2O mixture (8 mL). To this solution was added Hmte (156 μL, 1.80 mmol). The mixture was refluxed under argon for 9 h in the dark, after which it was filtered hot over celite. Acetone was removed under reduced pressure upon which the crude product with PF_6^- counter ions precipitated in water. It was filtered, washed and dried. PF_6^- ions were exchanged by Cl^- by stirring a 1:1 acetone/water solution (20 mL) of the crude product [**2**]$(PF_6)_3$ with ion-exchange resin DOWEX 22 (30 mg) for 4 h. After filtration of the resin, acetone was evaporated under reduced pressure, and water was removed using a freeze drier machine to afford [**2**]Cl_3 as a reddish purple powder (12 mg, 0.011 mmol, 43%). ^{1}H

NMR (300 MHz, CD_3OD, 298 K, *see Figure S5 for proton attribution*) δ (ppm) 9.80 (d, J = 6.1 Hz, 1H, 6A), 8.81 (d, J = 8.1 Hz, 1H, 3A), 8.57 (t, J = 8.7 Hz, 2H, 1R' + 3B), 8.39 (m, 2H, 10R' + 4A), 8.0-8.05 (m, 4H, 5R + 9R'+ 7R' + 5A), 7.93 (t, 2H, 4B + 2R'), 7.86 – 7.73 (m, 5H, 3R + T33''+ T3'+ T5'), 7.56 (m, 1H, 2R), 7.48 – 7.32 (m, 4H, 4R'+ 4R + T4 + T4''), 7.27 (d, J = 7.2 Hz, 1H, 5B), 7.20 – 7.07 (m, 3H, 6B + T55''), 6.92 (d, J = 4.1 Hz, 2H, T6 + T6''), 4.46 (d, J = 5.5 Hz, 2H, α), 3.80 (t, 2H, β), 3.69 (q, 8H, δ), 3.46(d, J = 5.7 Hz, 2H, HO-$\underline{CH_2}$), 3.25 (s, 3H, γ), 1.81 (t, J = 5.8 Hz, 2H, $\underline{CH_2}$-S), 1.43 – 1.36 (s, 3H, S-$\underline{CH_3}$), 1.28 (t, J = 6.9 Hz, 12H, *ε*). ^{13}C NMR (75 MHz, CD_3OD, 298 K) δ (ppm) 173.90 (C=O), 168.19 (3R,8R), 159.51, 159.34, 159.30, 159.12, 158.99, 158.96, 157.22, 154.52 (6A), 153.41, 140.05, 139.95, 139.09, 137.18, 135.81, 135.50, 133.83, 133.34, 133.24, 131.33, 131.16, 129.59, 128.90, 127.22, 126.20, 125.81, 124.98, 115.35, 114.86, 112.95, 97.32, 60.46 (α), 47.05 (β), 46.10 (δ), 46.08 (S-$\underline{C}H_3$), 39.53 (γ), 38.51 (OH-$\underline{C}H_2$), 38.08($\underline{C}$H2-S), 12.83 (*ε*). High resolution ES MS m/z (calc): 360.45788 (360.45780 $[M–3Cl]^{3+}$), 540.18291 (540.18289 $[M–3Cl–H]^{2+}$). UV-vis*:* λ_{max} (ε in $L\cdot mol^{-1}\cdot cm^{-1}$) in pure H_2O: 570 nm (44×10^3).

Emission measurements. Three stock solutions of rhodamine B (solution **C**, 2.4 mg in 50 mL H_2O, 1.0×10^{-4} M), of compound [**4**]Cl (solution **B**, 3.8 mg in 50 mL H_2O, 1.0×10^{-4} M) and of compound [**2**]Cl_3 (solution **C**, 1.2 mg in 10 mL H_2O, 1.0×10^{-4} M) were prepared. 150 µL of stock solution **A**, 100 µL of solution **B,** or 120 µL of solution **C** was transferred into a quartz cuvette and was diluted to 3 mL by adding H_2O using a micropipette (final concentrations: of **A'**: 5.0×10^{-6} M, **B'**: 3.3×10^{-6} M, **C'**: 4.0×10^{-6} M). The absorbance of each solution was measured (A_{570}=0.23 for all solutions). Emission spectra were recorded with the same excitation parameters (λ_e=570 nm).

Calculation of the emission quantum yield for [4]Cl. The relative method was applied to obtain the emission quantum yield of [**4**]Cl (φ_4). Rhodamine B was used as a reference sample (φ_{ref}=0.31 in water).[38] The emission spectra of Rhodamine B and [**4**]Cl were recorded

in optically diluted aqueous solutions ($A_{570} \leq 0.1$); the integrated intensities of the emission spectra, D_{ref} and D_4, respectively, were calculated, to afford the emission quantum yield of [**4**]Cl, φ_4, according to the equation:

$$\varphi_4 = \varphi_{ref} \cdot \left(\frac{D_4}{D_{ref}}\right) \cdot \left(\frac{A_{ref}}{A_4}\right)$$

where A is the absorbance at the excitation wavelength (λ_e=*570* nm). The subscripts *ref* and *4* refer to the reference (Rhodamine B) and measured sample ([**4**]Cl), respectively. The value found was φ_s=0.12(2).

Calculation of the Förster distance R_0 and Förster efficiency φ_{FRET} for the dyad [2]Cl$_3$. The Förster distance R_0 (in Å) for the FRET couple made of a rhodamine donor (modeled as [**4**]$^+$) and a ruthenium acceptor (modeled as [**1**]$^{2+}$) was calculated using the equation:

$$R_0 = 9.78 \times 10^3 \cdot \left(k^2 \cdot n^{-4} \cdot \varphi_4 \cdot \int F_D(\lambda) \cdot \varepsilon_A(\lambda) \cdot \lambda^4 \cdot d\lambda\right)^{1/6}$$

where k^2 represents the relative orientation in space of the transition dipoles of the donor and acceptor (k^2=0.667), n is the reflective index of the solution (1.3), φ_4=0.12 is the emission quantum yield of the donor ([**4**]Cl) in absence of the acceptor, $F_D(\lambda)$ is the donor emission intensity at the wavelength λ, dimensionless, and normalized to an area of 1, and ε_A is the extinction coefficient of the ruthenium acceptor at the wavelength λ. In this equation the unit of λ and ε_A are cm and $cm^{-1} \cdot M^{-1}$, respectively. The overlap integral curve is shown in Figure S10, the overlap integral J_{DA} was 3.05×10^{-15} $cm^3.M^{-1}$, and R_0 was calculated to be 20.5 Å.

From the DFT model of the dyad [**2**]$^{3+}$ (see below) a distance *r=12.1* Å was found between the centroid of the central aromatic ring of rhodamine, and the nitrogen atom of the central pyridine ring of the terpyridine ligand. Using r as the distance between the donor and the acceptor in the dyad, a FRET efficiency φ_{FRET}=0.96 was calculated according to the equation:

$$\varphi_{FRET} = \frac{1}{(r/R_0)^6}$$

DFT calculation.

From the X-ray structure of [**1**]$(PF_6)_2$ a 3D model of the dyad [**2**]$^{3+}$ was build using the MOLDEN software.[50] An extended configuration of the linker was chosen to maximize the distance between the ruthenium and rhodamine fragments. The initial geometry was minimized by DFT using the B3LYP functional and LANL2DZ as the basis set for all elements as described in the GAMESS-UK package.[51] In the final geometry the centroid Cg1 of the C76-C77-C82-O83-C84-C136 aromatic ring was calculated using Mercury from CCDC, and the Cg1-N8 distance was measured to be *r=12.1* Å. All X,Y,Z coordinates of the minimized structure are given in the Supplementary Information, and a picture of the model prepared with MOLDEN is given as Figure S11.

Irradiation experiments

NMR measurements. [**2**]Cl_3 (3.8 mg, 3.2 μmol) was weighed into an NMR tube and degassed D_2O (0.60 mL) was added to the tube in the dark under argon. The ^{1}H NMR of the sample was measured as a reference, and irradiation at 452 nm or 570 nm was started at T=298 K using the beam of a LOT 1000 W Xenon arc lamp filtered with an Andover filter at the appropriate wavelength, and arriving on the side of the NMR tube (see *supporting Information, Figure S9*). After 220 minutes, 310 minutes, and 480 minutes of irradiation at 452 nm, or 170 minutes, 320 minutes, and 530 minutes at 570 nm, ^{1}H NMR spectra were measured. A reference sample was also prepared at the same concentration, and kept in the dark for comparison of their ^{1}H NMR spectra. Neither of these reference samples showed any observable conversion in the dark.

UV-vis experiments. 1 mL of a stock solution **D** of compound [**2**]Cl_3 (1.2 mg in 10 mL H_2O, 1.0×10^{-4} M) or 0.8 mL of a stock solution **E** of [**1**]$(BF_4)_2$ (1.7 mg in 5 mL H_2O, 4.5×10^{-4} M) was transferred into a UV-vis cuvette. The volume of the solution was completed to 3 mL with H_2O (using a micropipette) in the dark (final concentration: **D'**: 3.4×10^{-5} M, **E'**: $1.2\times10^{-}$

^{4} M). The UV-vis spectrum of each sample was measured and afterwards the sample was irradiated at 452 nm or 570 nm using the beam of a LOT 1000 W Xenon arc lamp filtered by an Andover bandpath filter, and directed into an 2.5 mm diameter optical fiber bundle bringing the light vertically into the cuvette, *i.e,* perpendicular to the horizontal optical axis of the spectrophotometer (*see Supporting Information, Figure S8)*. After each irradiation period (varying from 1 min to 3 min depending on the samples) a UV-vis spectrum was measured until a total irradiation time of 350 minutes and 82 minutes was reached, for **D'** and **E'**, respectively. The concentrations in *[RuHmte]* ([**2**]$^{3+}$ or [**1**]$^{2+}$) and [$RuOH_2$] ([**7**]$^{3+}$ or [**8**]$^{2+}$) were determined by deconvolution knowing the extinction coefficients of both species (*see Supporting Information*). The evolution of $ln([RuHmte]/[Ru]_{tot})$ was plotted as a function of irradiation time, and from the slope S of these plot k_{φ} at λ_e=452 nm or λ_e=570 nm were determined to be 1.9(3)×10^{-4} s^{-1} and 4.4(3)×10^{-4} s^{-1}, for [**2**]$^{3+}$, respectively, and 1.3(4)×10^{-4} and 5.2(2)×10^{-5} s^{-1} for [**1**]$^{2+}$, respectively. Knowing the photon flux and probability of photon absorption $1-10^{-Ae}$, where A_e is the absorbance of the solution at the excitation wavelength λ_e, the number of moles of photons Q absorbed at time t by RuHmte since t_{irr}=0 was calculated. Plotting n_{RuHmte} (the number of moles of RuHmte complex [**1**]$^{2+}$ or [**2**]$^{3+}$) *vs.* Q gave a straight line in each case. The slope of this plot directly corresponds to the quantum yield of the photosubstitution reaction. The values for the photosubstitution quantum yields were 9.2(3) ×10^{-3} and 8.5(3)×10^{-3}, respectively, for [**2**]$^{3+}$ and 1.6(4)×10^{-2} and 1.1(4)×10^{-2}, respectively, for [**1**]$^{2+}$, at λ_e=452 nm or λ_e=570 nm, respectively (*see Supporting Information).*

Acknowledgements

NWO-CW is kindly acknowledged for a Veni grant to S.B. Prof. E. Bouwman is also wholeheartedly acknowledged for fruitful scientific discussions and support.

References

1. C. R. Hecker, P. E. Fanwick and D. R. McMillin, *Inorg. Chem.*, 1991, **30**, 659-666.
2. V. Balzani, G. Bergamini, S. Campagna and F. Puntoriero, in *Photochemistry and Photophysics of Coordination Compounds I*, ed. V. C. S. Balzani, 2007, vol. 280, pp. 1-36.
3. B. A. McClure, E. R. Abrams and J. J. Rack, *J. Am. Chem. Soc.*, 2010, **132**, 5428-5436.
4. P. S. Wagenknecht and P. C. Ford, *Coord. Chem. Rev.*, 2011, **255**, 591-616.
5. E. Baranoff, J. P. Collin, J. Furusho, Y. Furusho, A. C. Laemmel and J. P. Sauvage, *Inorg. Chem.*, 2002, **41**, 1215-1222.
6. A. A. Rachford and J. J. Rack, *J. Am. Chem. Soc.*, 2006, **128**, 14318-14324.
7. S. Bonnet, J. P. Collin, J. P. Sauvage and E. Schofield, *Inorg. Chem.*, 2004, **43**, 8346-8354.
8. P. Mobian, J. M. Kern and J. P. Sauvage, *Angew. Chem. Int. Ed.*, 2004, **43**, 2392-2395.
9. J. Van Houten and R. J. Watts, *J. Am. Chem. Soc.*, 1976, **98**, 4853-4858.
10. P. C. Ford, *Coord. Chem. Rev.*, 1982, **44**, 61-82.
11. S. Bonnet and J.-P. Collin, *Chem. Soc. Rev.*, 2008, **37**, 1207-1217.
12. R. B. Sears, L. E. Joyce, M. Ojaimi, J. C. Gallucci, R. P. Thummel and C. Turro, *J. Inorg. Biochem.*, 2013, **121**, 77-87.
13. B. S. Howerton, D. K. Heidary and E. C. Glazer, *J. Am. Chem. Soc.*, 2012, **134**, 8324-8327.
14. R. N. Garner, J. C. Gallucci, K. R. Dunbar and C. Turro, *Inorg. Chem.*, 2011, **50**, 9213-9215.
15. S. Betanzos-Lara, L. Salassa, A. Habtemariam, O. Novakova, A. M. Pizarro, G. J. Clarkson, B. Liskova, V. Brabec and P. J. Sadler, *Organometallics*, 2012, **31**, 3466-3479.
16. A. J. Gomes, P. A. Barbougli, E. M. Espreafico and E. Tfouni, *J. Inorg. Biochem.*, 2008, **102**, 757-766.
17. F. Barragan, P. Lopez-Senin, L. Salassa, S. Betanzos-Lara, A. Habtemariam, V. Moreno, P. J. Sadler and V. Marchan, *J. Am. Chem. Soc.*, 2011, **133**, 14098-14108.
18. R. E. Goldbach, I. Rodriguez-Garcia, J. H. van Lenthe, M. A. Siegler and S. Bonnet, *Chem. Eur. J.*, 2011, **17**, 9924-9929.
19. N. J. Farrer, L. Salassa and P. J. Sadler, *Dalton Trans.*, 2009, 10690-10701.
20. H. M. Chen, J. A. Parkinson, S. Parsons, R. A. Coxall, R. O. Gould and P. J. Sadler, *J. Am. Chem. Soc.*, 2002, **124**, 3064-3082.
21. D. Crespy, K. Landfester, U. S. Schubert and A. Schiller, *Chem. Commun.*, 2010, **46**, 6651-6662.
22. A. Juarranz, P. Jaen, F. Sanz-Rodriguez, J. Cuevas and S. Gonzalez, *Clin. Transl. Oncol.*, 2008, **10**, 148-154.
23. A. P. Castano, P. Mroz and M. R. Hamblin, *Nat. Rev. Cancer*, 2006, **6**, 535-545.
24. A. M. Bugaj, *Photochem. Photobiol. Sci.*, 2011, **10**, 1097-1109.
25. P. Zhang, W. Steelant, M. Kumar and M. Scholfield, *J. Am. Chem. Soc.*, 2007, **129**, 4526-4527.
26. R. Weissleder and V. Ntziachristos, *Nat. Med.*, 2003, **9**, 123-128.
27. S. L. H. Higgins and K. J. Brewer, *Angew. Chem. Int. Ed.*, 2012, **51**, 11420-11422.
28. M. J. Rose, M. M. Olmstead and P. K. Mascharak, *J. Am. Chem. Soc.*, 2007, **129**, 5342-+.

29. M. J. Rose, N. L. Fry, R. Marlow, L. Hinck and P. K. Mascharak, *J. Am. Chem. Soc.*, 2008, **130**, 8834-8846.
30. N. L. Fry, J. Wei and P. K. Mascharak, *Inorg. Chem.*, 2011, **50**, 9045-9052.
31. N. L. Fry and P. K. Mascharak, *Acc. Chem. Res.*, 2011, **44**, 289-298.
32. J. P. Sauvage, J. P. Collin, J. C. Chambron, S. Guillerez, C. Coudret, V. Balzani, F. Barigelletti, L. Decola and L. Flamigni, *Chem. Rev.*, 1994, **94**, 993-1019.
33. K. Sienicki and W. L. Mattice, *J. Chem. Phys.*, 1989, **90**, 6187-6192.
34. P. Woolley, K. G. Steinhauser and B. Epe, *Biophys. Chem.*, 1987, **26**, 367-374.
35. M. H. Lim and S. J. Lippard, *Inorg. Chem.*, 2004, **43**, 6366-6370.
36. E. K. Kainmuller, E. P. Olle and W. Bannwarth, *Chem. Commun.*, 2005, 5459-5461.
37. M.-J. Li, K. M.-C. Wong, C. Yi and V.-W. Yam, *Chem. Eur. J.*, 2012, **18**, 8724-8730.
38. O. Filevich, B. Garcia-Acosta and R. Etchenique, *Photochem. Photobiol. Sci.*, 2012, **11**, 843-847.
39. A. Bahreman, B. Limburg, M. A. Siegler, E. Bouwman and S. Bonnet, *Inorg. Chem.*, 2013, **52**, 9456-9469.
40. H. N. Kim, M. H. Lee, H. J. Kim, J. S. Kim and J. Yoon, *Chem. Soc. Rev.*, 2008, **37**, 1465-1472.
41. M. Beija, C. A. M. Afonso and J. M. G. Martinho, *Chem. Soc. Rev.*, 2009, **38**, 2410-2433.
42. S. Burazerovic, J. Gradinaru, J. Pierron and T. R. Ward, *Angew. Chem. Int. Ed.*, 2007, **46**, 5510-5514.
43. J. del Marmol, O. Filevich and R. Etchenique, *Anal. Chem.*, 2010, **82**, 6259-6264.
44. R. A. Leising, S. A. Kubow, M. R. Churchill, L. A. Buttrey, J. W. Ziller and K. J. Takeuchi, *Inorg. Chem.*, 1990, **29**, 1306-1312.
45. C. A. Bessel, J. A. Margarucci, J. H. Acquaye, R. S. Rubino, J. Crandall, A. J. Jircitano and K. J. Takeuchi, *Inorg. Chem.*, 1993, **32**, 5779-5784.
46. M.-P. Santoni, A. K. Pal, G. S. Hanan, A. Proust and B. Hasenknopf, *Inorg. Chem. Commun.*, 2011, **14**, 399-402.
47. M. Kasha, *Discuss. Faraday Soc.*, 1950, 14-19.
48. A. Bahreman, B. Limburg, M. A. Siegler, R. Koning, A. J. Koster and S. Bonnet, *Chem. Eur. J.*, 2012, **18**, 10271-10280.
49. E. C. Constable and M. D. Ward, *Dalton Trans.*, 1990, 1405-1409.
50. G. Schaftenaar and J. H. Noordik, *J. Comput-Aided. Mol. Des.*, 2000, **14**, 123-134.
51. M. F. Guest, I. J. Bush, H. J. J. Van Dam, P. Sherwood, J. M. H. Thomas, J. H. Van Lenthe, R. W. A. Havenith and J. Kendrick, *Mol. Phys.*, 2005, **103**, 719-747.